




## Article

# Novel Neural Network Optimized by Electrostatic Discharge Algorithm for Modification of Buildings Energy Performance

Arash Mohammadi Fallah <sup>1</sup>, Ehsan Ghafourian <sup>2</sup>, Ladan Shahzamani Sichani <sup>3</sup>, Hossein Ghafourian <sup>4</sup>, Behdad Arandian <sup>5</sup> and Moncef L. Nehdi <sup>6,\*</sup>

<sup>1</sup> Department of Architecture, Urmia Branch, Islamic Azad University, Urmia 5719976453, Iran

<sup>2</sup> Department of Computer Science, Iowa State University, Ames, IA 50010, USA

<sup>3</sup> Department of Art and Architecture, Semirom Branch, Islamic Azad University, Semiron 7357586619, Iran

<sup>4</sup> Department of Civil and Environmental Engineering, University of Massachusetts Amherst, Amherst, MA 01375, USA

<sup>5</sup> Department of Electrical Engineering, Dolatabad Branch, Islamic Azad University, Isfahan 8194975178, Iran

<sup>6</sup> Department of Civil Engineering, McMaster University, Hamilton, ON L8S 4L8, Canada

\* Correspondence: nehdim@mcmaster.ca

**Abstract:** Proper analysis of building energy performance requires selecting appropriate models for handling complicated calculations. Machine learning has recently emerged as a promising effective solution for solving this problem. The present study proposes a novel integrative machine learning model for predicting two energy parameters of residential buildings, namely annual thermal energy demand ( $D_{THE}$ ) and annual weighted average discomfort degree-hours ( $H_{DD}$ ). The model is a feed-forward neural network (FFNN) that is optimized via the electrostatic discharge algorithm (ESDA) for analyzing the building characteristics and finding their optimal contribution to the  $D_{THE}$  and  $H_{DD}$ . According to the results, the proposed algorithm is an effective double-target model that can predict the required parameters with superior accuracy. Moreover, to further verify the efficiency of the ESDA, this algorithm was compared with three similar optimization techniques, namely atom search optimization (ASO), future search algorithm (FSA), and satin bowerbird optimization (SBO). Considering the Pearson correlation indices 0.995 and 0.997 (for the  $D_{THE}$  and  $H_{DD}$ , respectively) obtained for the ESDA-FFNN versus 0.992 and 0.938 for ASO-FFNN, 0.926 and 0.895 for FSA-FFNN, and 0.994 and 0.995 for SBO-FFNN, the ESDA provided higher accuracy of training. Subsequently, by collecting the weights and biases of the optimized FFNN, two formulas were developed for easier computation of the  $D_{THE}$  and  $H_{DD}$  in new cases. It is posited that building engineers and energy experts could consider the use of ESDA-FFNN along with the proposed new formulas for investigating the energy performance in residential buildings.

**Keywords:** optimization; sustainable energy; building energy performance; thermal load



**Citation:** Fallah, A.M.; Ghafourian, E.; Shahzamani Sichani, L.; Ghafourian, H.; Arandian, B.; Nehdi, M.L. Novel Neural Network Optimized by Electrostatic Discharge Algorithm for Modification of Buildings Energy Performance. *Sustainability* **2023**, *15*, 2884. <https://doi.org/10.3390/su15042884>

Academic Editor: Antonio Caggiano

Received: 24 December 2022

Revised: 2 February 2023

Accepted: 3 February 2023

Published: 5 February 2023



**Copyright:** © 2023 by the authors. Licensee MDPI, Basel, Switzerland. This article is an open access article distributed under the terms and conditions of the Creative Commons Attribution (CC BY) license (<https://creativecommons.org/licenses/by/4.0/>).

## 1. Introduction

As a well-known objective of many research efforts, engineers have tried to address complex problems using new scientific developments and emerging computational tools [1–3]. In this way, they have focused on solving newly risen issues, as well as improving previous solutions (e.g., maximizing efficiency [4–6]). These strategies can be classified as laboratory measurements, computer-based simulations, numerical and empirical calculations, soft computing, and artificial intelligence techniques, etc.

Buildings, as a primary residence for people and location of governmental and private entities and industries, are receiving large attention from the perspective of both consumers and authorities [7–9]. With the advances in the economy and population growth, buildings are consuming a noticeable share of the total energy worldwide [10,11]. This excess consumption is associated with adverse effects such as air pollutant emissions which itself can impact human health (e.g., respiratory and heart diseases) and cause climate

change and global warming issues [12–14]. These effects call for investigating the buildings energy performance and developing ideas for enhancing it.

This issue has formed the motivation of many recent studies to look for efficient and effective evaluative methods for approximating the building's behavior in terms of energy consumption [13,15]. Among a wide variety of methods suggested for this purpose, machine learning tools have received considerable attention. These methods propose accurate and inexpensive approaches for analyzing the energy parameters in buildings with various usages (e.g., predicting required thermal loads [16,17]).

The advent of new computational approaches like artificial intelligence has highly influenced the world of science [18,19]. Programming experts have so far introduced a wide variety of machine learning techniques for prediction purposes [20,21]. Famous models rely on theories such as neuro-fuzzy, support vector, and tree-based approaches for training the network and attaining a reliable understanding of the intended parameters. Artificial neural networks (ANNs) [22] are another well-known set of algorithms that contribute to an extensive range of machine learning applications. These models have also shown high promise for simulating different energy parameters [23–25]. Energy performance included, many authors have applied ANN-based techniques for analyzing the buildings characteristics towards predicting the required energies such as thermal loads [26]. In this process, the network receives the building's characteristics including dimensions, glazing, positions, etc., and performs neural calculations to establish the best relationship between these factors and the parameters of interest.

The training process in machine learning models is conducted by specific algorithms that are embedded in the model. Apart from typical training algorithms, recent studies have proposed the use of sophisticated optimization techniques for this purpose. These algorithms are known as population-based metaheuristic techniques that are mostly inspired by nature [27,28]. The application of metaheuristic algorithms in combination with various machine learning models, covers a wide range of subjects including building energy performance [29–31]. For instance, Alkhazaleh, et al. [32] applied a machine learning adaptive neuro-fuzzy-inference system (ANFIS) to predict building energy demand. The ANFIS was trained using equilibrium optimization (EO), Harris hawks optimization (HHO), grey wolf optimizer (GWO), and slap swarm algorithm (SSA), and a comparison among them revealed the better capability of the first two algorithms for this task.

Earlier generations of metaheuristic techniques comprise algorithms like particle swarm optimization, genetic algorithm, imperialist competitive algorithm, etc. that have effectively served for optimizing intelligent models in predicting energy parameters such as building thermal loads [33,34]. On the other hand, many similar studies have reported the excellent optimization ability of the newer members of this family as well [35,36]. Hence, this promotes the need for continual testing of recent algorithms to keep the solution of energy problems updated with methodological advances.

Existing literature indicates that intelligent models like ANNs are very suitable for analyzing the energy performance of various types of buildings. On the other hand, it was stated that the performance of these models can be optimized when they are associated with appropriate metaheuristic optimizers. Based on these advantages, this work pursues three pivotal objectives:

- (i) A new methodology, based on the combination of feed-forward neural network (FFNN) and a metaheuristic technique called electrostatic discharge algorithm (ESDA), is proposed for energy performance analysis in residential buildings. This task is carried out by predicting annual thermal energy demand ( $D_{THE}$ ) and annual weighted average discomfort degree-hours ( $H_{DD}$ ) by analyzing the building's architecture. Notably, the FFNN is one of the most capable neural predictors that supports double-target prediction, i.e., simultaneous prediction of two parameters [37]. Likewise, the ESDA is among the powerful metaheuristic optimizers that have successfully optimized FFNN for different purposes such as predicting electrical power [38],

- footing bearing capacity [39], and more relevantly optimizing heating, ventilation and air-conditioning (HVAC) systems [36].
- (ii) A comparison is conducted among the ESDA and similar algorithms to comparatively validate the performance of the suggested model. The benchmark algorithms are the future search algorithm (FSA) [40], atom search optimization (ASO) [41], and satin bowerbird optimization (SBO) [42]. In such studies, due to the performance of several algorithms, the main solution is excerpted among numerous candidates, which increases the reliability of solving the problem.
  - (iii) Knowing that a reliable early approximation of the required thermal load of a building can be very beneficial, the methodology presented in this study can contribute to practical applications such as optimizing relevant designs (e.g., building characteristics and energy systems).

## 2. Materials and Methods

### 2.1. Data Provision

In order for the machine learning model to implement the prediction task, a dataset is prepared. The dataset is the analysis result of a residential building in Marrakech (Morocco) which was carried out in transient system simulation tool (TRNSYS) environment [43] based on a study by Chegari, et al. [44]. The used package, associated with appropriate standards, enables experts to perform energy analysis of a building by using its characteristics such as geometry, thermo-physical parameters, orientation, etc. The main outcomes of the analysis were two energy parameters:

- (i) DThE (annual thermal energy demand): calculated as the sum of heating and cooling loads over the building's total conditioned area,
- (ii) HDD (annual weighted average discomfort degree-hours): calculated as the annual weighted average of the degree-hours, during which, the resident feels uncomfortable where he/she should feel more comfortable.

Further details regarding the simulation conditions and relevant assumptions can be found in the reference paper [44].

Overall, the dataset is composed of thirteen factors, classified as two target factors:

- (a) DThE in  $\text{kWh}\cdot\text{m}^{-2}\cdot\text{year}^{-1}$
- (b) HDD in  $^{\circ}\text{C}\cdot\text{h}\cdot\text{year}^{-1}$
- (c) and eleven input factors given below:
- (d) Transmission coefficient of the external walls (UM) in  $\text{W}\cdot\text{m}^{-2}\cdot\text{K}^{-1}$
- (e) Transmission coefficient of the roof (UT) in  $\text{W}\cdot\text{m}^{-2}\cdot\text{K}^{-1}$
- (f) Transmission coefficient of the floor (UP) in  $\text{W}\cdot\text{m}^{-2}\cdot\text{K}^{-1}$
- (g) Solar radiation absorption coefficient of the exterior walls ( $\alpha\text{M}$ ),
- (h) Solar radiation absorption coefficient of the roof ( $\alpha\text{T}$ ),
- (i) Linear coefficient of thermal bridges (Pt) in  $\text{W}\cdot\text{m}^{-1}\cdot\text{K}^{-1}$ ,
- (j) Air change rate (RA-CH) in  $\text{v}\cdot\text{h}^{-1}$ ,
- (k) Shading coefficient of North-facing windows (ShCW-N),
- (l) Shading coefficient of South-facing windows (ShCW-S),
- (m) Shading coefficient of East-facing windows (ShCW-E), and
- (n) Glazing (GZ).

The correlation matrix of the used dataset is illustrated in Figure 1. The main diagonal of this matrix shows the histogram of the factors (e.g., the first element on the main diagonal shows the histogram of the  $U_M$ ). Other elements are depicted in scatter charts showing the relationship between the corresponding factor and the other twelve factors. Also, the reported value expresses the correlation between two factors in each chart. According to the last two rows of this matrix, the  $D_{\text{ThE}}$  is meaningfully correlated with all input factors, while the  $H_{\text{DD}}$  is not so.

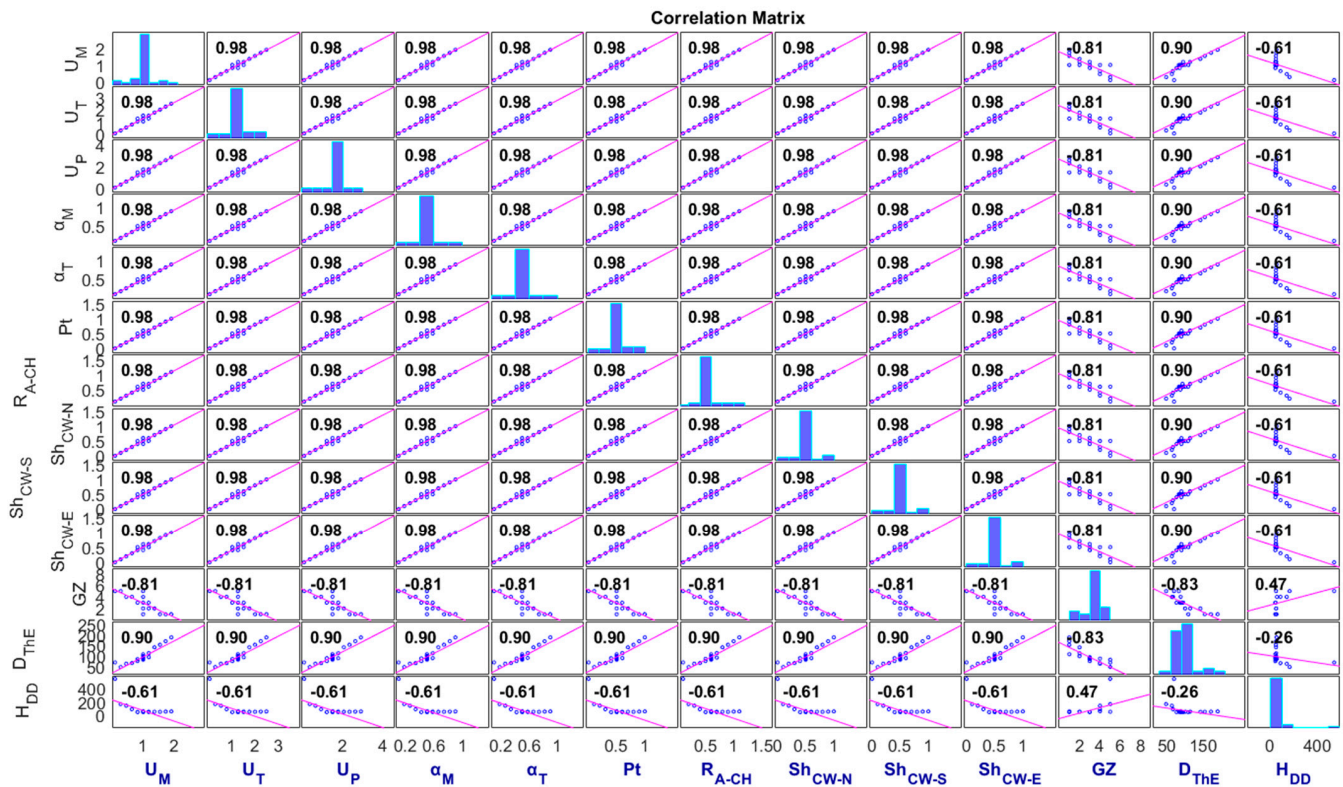


Figure 1. Scatter and histogram charts of the dataset factors.

Moreover, the dataset was statistically analyzed in Excel environment through Data Analysis Section—Descriptive Statistics tool. Table 1 presents the results of this process.

Table 1. Dataset statistical assessment results.

Type	Factor	Mean	Standard Deviation	Sample Variance	Minimum	Maximum
Inputs	$U_M$ ( $W.m^{-2}.K^{-1}$ )	1.00	0.33	0.11	0.10	1.90
	$U_T$ ( $W.m^{-2}.K^{-1}$ )	1.30	0.44	0.19	0.10	2.50
	$U_P$ ( $W.m^{-2}.K^{-1}$ )	1.50	0.51	0.26	0.10	2.90
	$\alpha_M$ (-)	0.50	0.15	0.02	0.10	0.90
	$\alpha_T$ (-)	0.50	0.15	0.02	0.10	0.90
	$Pt$ ( $W.m^{-1}.K^{-1}$ )	0.51	0.18	0.03	0.01	1.00
	$R_{A-CH}$ ( $v.h^{-1}$ )	0.60	0.18	0.03	0.10	1.10
	$Sh_{CW-N}$ (-)	0.50	0.18	0.03	0.00	1.00
	$Sh_{CW-S}$ (-)	0.50	0.18	0.03	0.00	1.00
	$Sh_{CW-E}$ (-)	0.50	0.18	0.03	0.00	1.00
Targets	GZ (-)	2.94	1.00	1.00	1.00	5.00
	$D_{THE}$ ( $kWh.m^{-2}.year^{-1}$ )	96.15	27.92	779.72	48.19	188.94
	$H_{DD}$ ( $^{\circ}C.h.year^{-1}$ )	69.53	87.07	7580.95	44.55	546.98

A total of 35 samples constitutes the used dataset (size =  $35 \times 13$ ). For this research, it was split into two sub-sets with 28 and 7 samples for the training and testing operations, respectively. Calculating the ratios indicate that 80% of data is devoted to the training task,

while the testing task uses 20% of them. To have an equal data division, a random selection was applied here.

## 2.2. Electrostatic Discharge Algorithm

As is known, metaheuristic algorithms are mostly inspired by natural behaviors like animal foraging actions [45,46]. On the other hand, there are some of them which follow the famous rules of the physics world in order to perform the optimization (e.g., optics inspired optimization [47]). The ESDA algorithm is another member of the latter family that is developed inspired by the electrostatic discharge phenomenon [48]. In definition, two bodies with different levels of electrostatic potential share a charge [49].

The optimization using ESDA begins with generating a population. The capability of each individual in this population is determined by a fitness value that represents the individual's immunity. In each implementation (i.e., iteration) of the ESDA, three individuals are randomly taken into consideration for performing the discharge. Next, a random value is produced. Based on the value of this random number, two cases are possible:

- (a) If the random value is greater than 0.5, two individuals with positions  $x_1$  and  $x_2$  execute the discharge as follows:

$$x_{2_{new}} = x_2 + 2 \cdot \beta_1 \cdot (x_1 - x_2) \quad (1)$$

- (b) If the random value is smaller than 0.5,

$$x_{3_{new}} = x_3 + 2 \cdot \beta_2 \cdot (x_1 - x_3) + 2 \cdot \beta_3 \cdot (x_2 - x_3) \quad (2)$$

In the above equations,  $\beta_i$  ( $i = 1, 2, 3$ ) signify random values and  $x_{i_{new}}$  represents the new position of the individual  $i$ .

Following this, a comprehensive check is done by the algorithm to confirm that all individuals are inside the boundaries. Finally, another check identifies the individuals that have been through more than 3 discharges, because the algorithm must treat them as eliminated individuals and replace them with newly generated ones. The explained process is repeated for each iteration with new individuals and the outstanding solution (i.e., the best fitness) is thereby discovered [48].

## 2.3. Feed-Forward Neural Network and Used Structure

So far, different versions of ANNs have been proposed and used for diverse simulations. These models are simulated on the basis of natural neural networks in the human brain [22,50]. Hence, the interaction between neural components forms a consistent network that is able to recognize and learn the pattern in the data. As a feedforward network, the FFNNs are first fed by appropriate data and this data is processed as it moves forward within the network [51]. For instance, in the MLP ANNs, the output of layer  $i$  is the input for layer  $i + 1$  [52]. In the following, the mechanism of these networks is explained.

Figure 2 shows the configuration of the FFNN that is optimized by metaheuristic algorithms in this research. As is seen, this network is composed of three layers:

- (i) Input layer which is fed by receiving eleven inputs of the dataset.
- (ii) Hidden layer which processes them.
- (iii) Output layer which releases the DThE and HDD.

In this figure, each blue circle represents a computational unit of the FFNN which are 11, 6, and 2 in the first, second, and third layers, respectively. Throughout the network, the neurons are forwardly connected using black arrows (named weights). Also, red arrows are considered as the bias of calculations (B stands for bias). Note that in the training of an FFNN, these weights and biases are adjusted and improved several times until meeting a stopping criterion. Thus, the ESDA algorithm is responsible for tuning these variables to create the best contribution from the  $U_M$ ,  $U_T$ ,  $U_P$ ,  $\alpha_M$ ,  $\alpha_T$ , Pt,  $R_{A-CH}$ ,  $Sh_{CW-N}$ ,  $Sh_{CW-S}$ ,  $Sh_{CW-E}$ , GZ to the  $D_{ThE}$ , and  $H_{DD}$ .

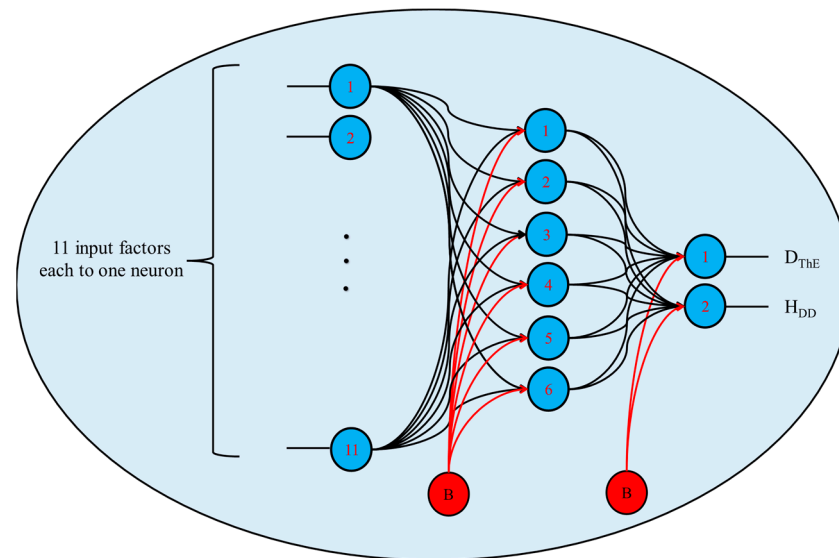


**Figure 2.** The ANN topology.

### 3. Results and Discussion

The pivotal objective of conducting this study is to examine the suitability of the FFNN-ESDA algorithm for predicting two parameters related to the energy performance of residential buildings. After model creation and data arrangement, the results are presented and discussed in the following parts.

The prediction reliability of the models is assessed in two phases:

- (i) Training phase during which the models acquire the knowledge of relationship between the D<sub>ThE</sub> and HDD with eleven input factors. A pattern is finally created in this phase using the training dataset.
- (ii) Testing phase for assessing the accuracy of the developed pattern.

In order to do these accuracy assessments, well-known accuracy criteria of root mean square error (RMSE), mean absolute error (MAE), and Pearson correlation coefficient ( $R_p$ ) are employed. Equations (3)–(5) express how these criteria are calculated.

$$RMSE = \sqrt{\frac{1}{K} \sum_{i=1}^K [(Q_{i_{expect}} - Q_{i_{estimate}})]^2} \quad (3)$$

$$MAE = \frac{1}{K} \sum_{i=1}^K |Q_{i_{expect}} - Q_{i_{estimate}}| \quad (4)$$

$$R_p = \frac{\sum_{i=1}^K (Q_{i_{estimate}} - \bar{Q}_{estimate}) (Q_{i_{expect}} - \bar{Q}_{expect})}{\sqrt{\sum_{i=1}^K (Q_{i_{estimate}} - \bar{Q}_{estimate})^2} \sqrt{\sum_{i=1}^K (Q_{i_{expect}} - \bar{Q}_{expect})^2}} \quad (5)$$

In the above equations,  $Q_{i_{expect}}$  represents the expected target values (i.e., real D<sub>ThE</sub> and real H<sub>DD</sub>),  $Q_{i_{estimate}}$  signifies the corresponding estimated values, and  $K$  shows the size of datasets which equals 28 in the training phase and 8 in the testing phase.

It is widely accepted that depending on the type of problem at hand (i.e., regression or classification problem) there are various statistical measures for evaluating the performance of machine learning models. In many similar works, utilizing a correlation index along with error criteria provided a reliable accuracy assessment for prediction tasks that use regression data [53–55], which is why the  $R_p$  is taken into consideration associated with two well-known error criteria (i.e., the RMSE and MAE). Specifically, while the RMSE and MAE

focus on the difference between the prediction and reality,  $R_p$  addresses the consistency of results by reporting a value in  $[0, 1]$ . Hereupon, smaller values of the RMSE and MAE, as well as greater values of  $R_p$ , demonstrate a better prediction.

### 3.1. Optimization

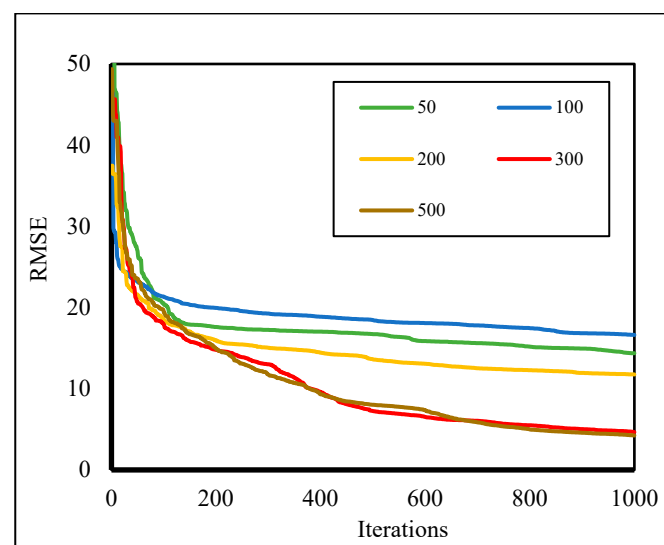
The first set of results is concerned with the optimization outcome. It was earlier mentioned that the ESDA, as well as FSA, ASO, and SBO, aim to provide the optimum weights and biases for the FFNN network. The steps below are taken for running a combination of the FFNN and the mentioned algorithms [56]:

- (i) Converting the FFNN into pure mathematical equations which predict the DThE and HDD, where the inputs are UM, UT, UP,  $\alpha M$ ,  $\alpha T$ , Pt, RA-CH, ShCW-N, ShCW-S, ShCW-E, and GZ.
- (ii) Determining an appropriate population size for each algorithm.
- (iii) Defining the number of iterations for each algorithm.
- (iv) Defining an objective function that measures the accuracy of training in each iteration.
- (v) Saving the best solution and constructing the final FFNN using optimized weights and biases.

The objective function for all models was the RMSE of training which is minimized to attain a better training. Since there are two outputs simultaneously predicted in this study, the objective function was set to be an average of the RMSE of both parameters, as expressed in the following equation:

$$\text{Objective function} = \frac{RMSE_{D_{ThE}} + RMSE_{H_{DD}}}{2} \quad (6)$$

However, due to different magnitudes of  $D_{ThE}$  and  $H_{DD}$ , their single RMSE was also controlled at the end of optimization. The number of iterations was 1000, based on the algorithms' behavior, while the population size was separately determined for each model after trying some relevant values. Figure 3a shows the results of this process for the ESDA algorithm with population size of 50–500. It was revealed that the ESDA, FSA, ASO, and SBO perform the best optimization when their population size is 300, 400, 400, and 400, respectively. Figure 3b illustrates the resulted optimization curves for the reported population sizes of the ESDA versus the benchmark algorithms. This figure gives important information from the optimization behavior of the algorithms such as initial and eventual error, convergence rate, and a comparison among the algorithms.



(a)

Figure 3. Cont.

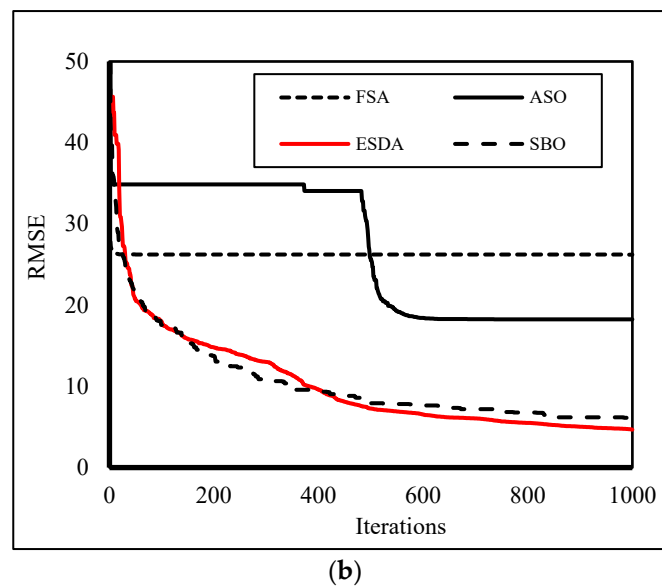


**Figure 3.** Optimization results in (a) different population sizes of the ESDA and (b) final curves for all algorithms.

### 3.2. Training and Results Assessment

The outcomes of the previous section are optimized (i.e., trained) FFNNs that have analyzed the training data to discover the non-linear relationship between the  $U_M$ ,  $U_T$ ,  $U_P$ ,  $\alpha_M$ ,  $\alpha_T$ ,  $P_t$ ,  $R_{A-CH}$ ,  $Sh_{CW-N}$ ,  $Sh_{CW-S}$ ,  $Sh_{CW-E}$ ,  $GZ$  with the  $D_{THE}$ , and  $H_{DD}$ . To examine the accuracy of this process, the predictions of the selected networks are compared one-by-one to the expected values. The goodness of these results indicates how good the models have been trained, while their performance when applied to testing data indicates a more important feature, namely generalizability. This feature answers the question “How is the accuracy of the models when they are applied to building conditions they never met before?”

For this purpose, using Equations (3)–(5), the error of prediction and correlation of results are measured for the training and testing datasets. Table 2 collects all calculated MAEs, RMSEs, and  $R_p$ s.

**Table 2.** The accuracy indicators obtained for predicting energy parameters.

Group	Algorithm	RMSE		MAE		$R_p$	
		$D_{THE}$	$H_{DD}$	$D_{THE}$	$H_{DD}$	$D_{THE}$	$H_{DD}$
Train	ESDA	2.53	6.79	1.70	4.04	0.995	0.997
	ASO	3.37	33.10	2.50	14.98	0.992	0.938
	FSA	10.58	41.84	6.70	26.17	0.926	0.895
	SBO	2.84	9.39	2.38	6.00	0.994	0.995
Test	ESDA	8.88	97.54	5.44	43.01	0.971	0.996
	ASO	8.28	72.16	6.06	37.16	0.983	0.990
	FSA	4.75	76.33	3.81	48.98	0.995	0.980
	SBO	8.93	90.59	6.03	41.91	0.970	0.996

For the  $D_{THE}$ , the training RMSEs of 2.53, 3.37, 10.58, and 2.84 are obtained for the FFNN model trained optimized with the ESDA, ASO, FSA, and SBO, respectively. The corresponding MAE values are 1.70, 2.50, 6.70, and 2.38. Concerning the testing phase, RMSEs are 8.88, 8.28, 4.75, and 8.93 along with the MAEs of 5.44, 6.06, 3.81, and 6.03.



All these results indicate that the errors of learning and prediction of the  $D_{ThE}$  are at an acceptable level.

As far as the  $R_p$  is concerned, Figure 4 depicts the regression charts of both training and testing data containing the correlation values. As it can be seen, all data points are well gathered around the “Best fit” line which represents an ideal prediction. Quantitatively speaking, the harmony between the expected and estimated  $D_{ThE}$  values are stated by the training  $R_p$ s 0.995, 0.992, 0.926, and 0.994 and testing  $R_p$ s 0.971, 0.983, 0.995, and 0.970.

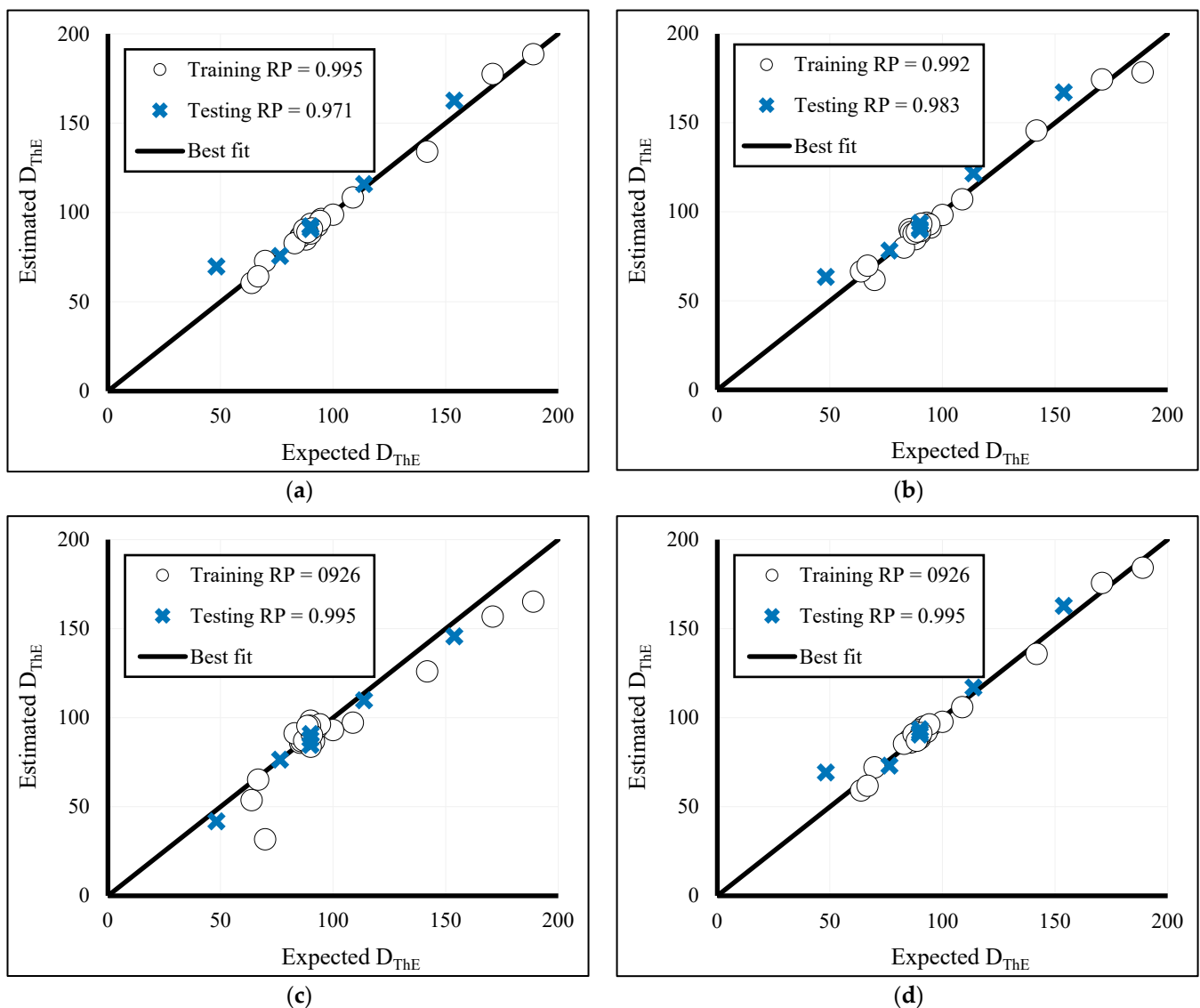


**Figure 4.** Correlation results for training and testing phases of the (a) ESDA, (b) ASO, (c) FSA, and (d) SBO corresponding to the  $D_{ThE}$ .

The same assessment is conducted for the  $H_{DD}$ . According to Table 2, training RMSEs 6.79, 33.10, 41.84, and 9.39, as well as the testing RMSEs 97.54, 72.16, 76.33, and 90.59 demonstrate a satisfying training. This claim can be supported by the training MAEs 4.04, 14.98, 26.17, and 6.00, as well as testing MAEs, 43.01, 37.16, 48.98, and 41.91.

Note that during optimization, an average of the training RMSEs obtained for the the  $D_{ThE}$  and  $H_{DD}$  determined the objective function of each iteration in Figure 3. Accordingly, the curves of the ESDA, ASO, FSA, and SBO ended up with values 4.66, 18.235, 26.21, and 6.115, respectively.

Figure 5 presents the correlation charts of the testing results. It is reported along with the charts that in the training phase, the  $R_p$ s are 0.997, 0.938, 0.895, and 0.995, and for the testing phase, 0.996, 0.990, 0.980, and 0.996. Both data groups (i.e., training and testing points) are nicely correlated around the “Best fit line”, which indicates the great accuracy of all models in predicting the  $H_{DD}$ .

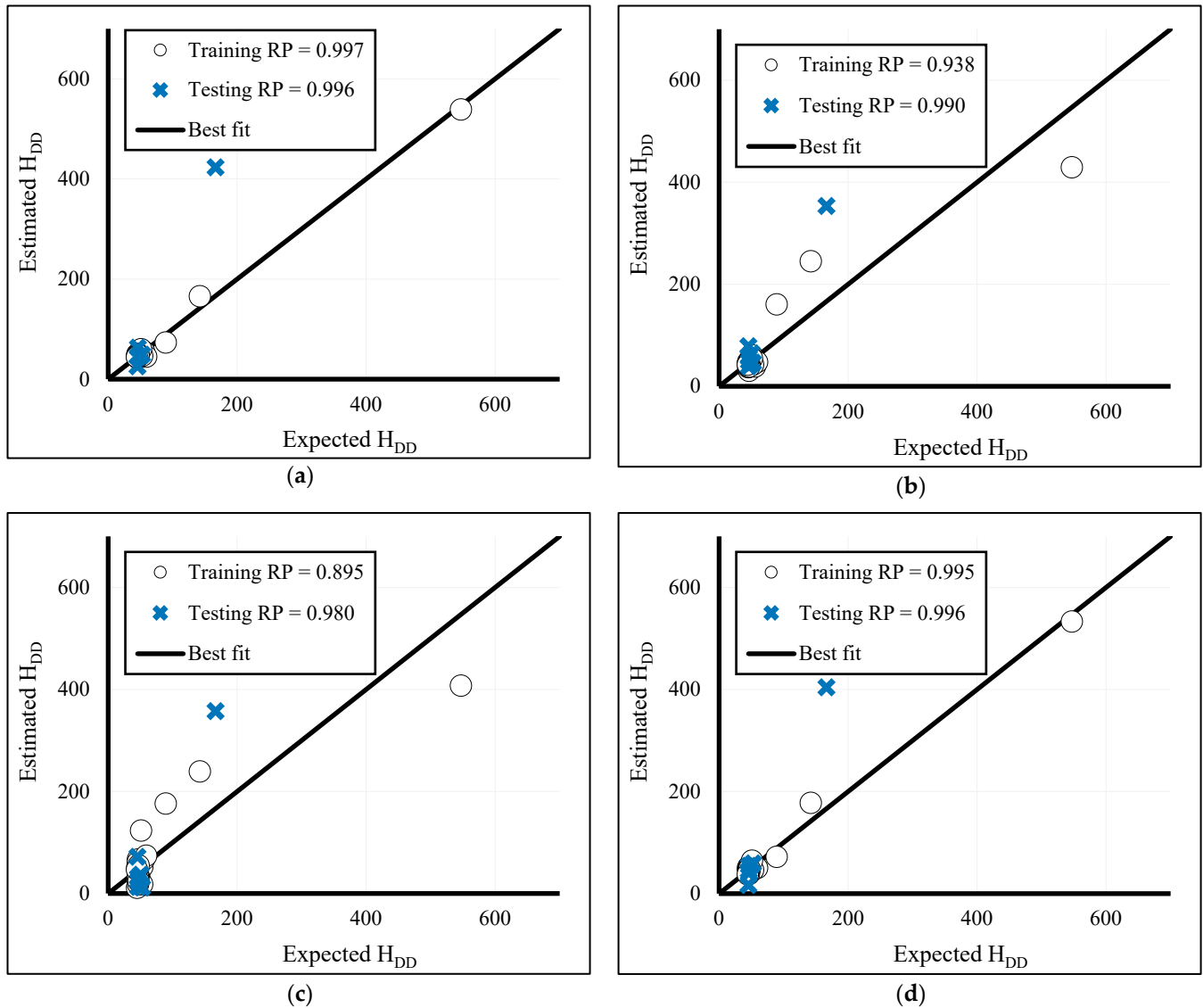


**Figure 5.** Correlation results for training and testing phases of the (a) ESDA, (b) ASO, (c) FSA, and (d) SBO corresponding to the  $H_{DD}$ .

### 3.3. Overall Assessment and Discussion

Along with buildings' analysis concerning civil/safety engineering [57–59], understanding the behavior of buildings in terms of required thermal load has economic and environmental advantages. It has been the motivation of many studies for developing sophisticated techniques to solve this problem. Recently, large attention has been paid to metaheuristic-optimized models, particularly newly developed algorithms. For example, the use of the symbiotic organism search algorithm for analyzing building thermal load was recommended by Rastbod, Rahimi, Dehghan, Kamranfar, Benjeddou and Nehdi [55]. This model also was found to outperform the political optimizer, harmony search algorithm, and backtracking search algorithms.

This study employed a powerful notion of these algorithms, i.e., the ESDA comparatively assessed with respect to ASO, FSA, and SBO. Based on the results given in the above section, it is shown that all models have been successful in analyzing the energy parameters of buildings. Hence, a significant finding can be the suitability of the ESDA, ASO, FSA, and SBO for training (i.e., optimizing) the FFNN. However, a comparative examination demonstrates that the performance of the ESDA was superior to three other algorithms. As explained in Section 2.2, a possible reason for this excellent optimization performance could be the strategy of eliminating exhausted individuals (i.e., those who experienced a certain number of discharges) and replacing them with new members [48]. The competency of this algorithm in optimizing FFNN has also been professed by scholars like Zhao and Foong [38] and Mu'azu [39]. After that, the SBO may stand as the second potential algorithm. It should be regarded that while the FSA was characterized with a weaker training compared to others, its testing results were quite promising.

Once again, due to the satisfying performance of the four models, a particularly the ESDA, in the training and testing phases, it is concluded that they are well capable of simultaneously understanding the  $D_{THE}$  and  $H_{DD}$  patterns, and also, reproducing these patterns for unseen building conditions. In almost all cases, the  $R_p$  values computed for the testing data were greater than 0.90, indicating above 90% agreement between the expected and estimated values.

Considering Figure 2, the analyzed network consisted of 86 variables (i.e., 78 weights + 8 biases) that were optimized consistently. What is quite clear is that adjusting such a bulky network should be a computer-supervised process and cannot be handled by humans. This study revealed that artificial intelligence can overcome this difficulty for good. As can be observed in Figure 3, each algorithm discarded 999 solutions to reach the optimal one in the 1000<sup>th</sup> iterations. Moreover, extensive trial and error efforts were executed to find the optimal population size for the algorithms (Section 3.1). Therefore, the obtained solutions are optimally selected among a wide range of candidates.

The FFNN used in this study was a double-target network that established a complicated relationship between two energy parameters (i.e.,  $D_{THE}$  and  $H_{DD}$ ) with eleven building characteristics. It enables the engineers and energy experts to use the applied methods for the early analysis of buildings. This advantage is helpful for the proper design of the building and relevant energy systems such as HVAC.

However, there are some potential ideas that may be considered for the following research efforts. Due to the large number of algorithms that are being developed for optimization objectives, the ESDA can be compared with further benchmarks in order to see whether the solution can be further enhanced. The experts may also make some improvements regarding the used data. As a limitation of this study, the dataset was restricted to 35 samples. Although the training was protected from undesirable phenomena such as local minima by the optimization algorithms, the models could extract reliable patterns, utilizing more datasets (e.g., the one used in [26,60]), which could be of interest for augmenting the generalizability of the models. Furthermore, developers may examine the effect of building characteristics which were  $U_M$ ,  $U_T$ ,  $U_P$ ,  $\alpha_M$ ,  $\alpha_T$ ,  $P_t$ ,  $R_{A-CH}$ ,  $Sh_{CW-N}$ ,  $Sh_{CW-S}$ ,  $Sh_{CW-E}$ , and  $GZ$  in this study, and decide on their importance in predicting the  $D_{THE}$  and  $H_{DD}$ . It can help to remove negligible parameters and reach a problem with smaller dimensions. This idea is further highlighted when it comes to double-target networks.

### 3.4. A Formula for Predicting Thermal Energy Demand and Discomfort Degree-Hours

An advantage of the FFNN-based model is that they can return a mathematical configuration of the trained network to act as a predictive formula [61,62]. To achieve the formula of the ESDA-FFNN model, the below steps are taken:

- (i) Extracting the weights and biases of the model
- (ii) Organizing the values into appropriate groups of weights and biases, as shown in Figure 2.

(iii) Calculating the outputs of the hidden layer by applying computations to the input vector as follows (see Figure 2):

$$\begin{bmatrix} A \\ B \\ C \\ D \\ E \\ F \end{bmatrix} = f \left( \begin{bmatrix} -0.3374 & -0.3282 & 0.1767 & 0.8781 & -0.4279 & -0.3241 & 0.2059 & 0.3453 & -0.0781 & -0.7531 & -0.6918 \\ -0.5812 & 0.3242 & -0.1861 & 0.0110 & -0.5952 & -0.0991 & -0.5579 & -0.4564 & -0.5107 & 0.5655 & 0.2792 \\ -0.0936 & 0.5428 & 0.3473 & -0.5375 & -0.1166 & -0.0359 & 0.2991 & -0.8096 & 0.4689 & 0.4012 & 0.2168 \\ -0.0936 & -0.4185 & 0.1311 & -0.5887 & -0.0719 & -0.0677 & -0.1671 & -0.5689 & 0.6790 & 0.1077 & 0.4722 \\ -0.1868 & -0.7452 & -0.6127 & 0.4716 & -0.4069 & -0.2226 & -0.1527 & 0.3231 & -0.3253 & 0.1171 & -0.3821 \\ 0.5834 & -0.4387 & 0.1087 & 0.3891 & -0.2620 & -0.3421 & 0.4136 & 0.5980 & 0.4451 & 0.6098 & -0.6202 \end{bmatrix} \times \begin{bmatrix} U_M \\ U_T \\ U_P \\ \alpha_M \\ \alpha_T \\ Pt \\ R_{A-CH} \\ Sh_{CW-N} \\ Sh_{CW-S} \\ Sh_{CW-E} \\ GZ \end{bmatrix} + \begin{bmatrix} 1.2748 \\ 0.9289 \\ 0.4346 \\ 0.0066 \\ -0.5169 \\ 2.5902 \end{bmatrix} \right), \quad (7)$$

where  $f(x)$  is a so-called “Tansig” activation function of the FFNN and is expressed as follows:

$$f(x) = \text{Tansig}(x) = \frac{2}{1 + e^{-2x}} - 1 \quad (8)$$

(iv) Giving the above produced values to the output layer to calculate the  $D_{THE}$  and  $H_{DD}$  (see Figure 2):

$$D_{THE} = -0.3740 \times A - 0.6589 \times B + 0.7669 \times C - 0.5731 \times D + 0.3722 \times E - 0.0999 \times F + 0.1832 \quad (9)$$

$$H_{DD} = 0.0921 \times A - 0.0355 \times B - 0.0056 \times C + 0.0073 \times D - 0.0151 \times E - 1.7295 \times F + 0.6601 \quad (10)$$

#### 4. Conclusions

This study reported a successful effort of employing a state-of-the-art computational technique for analyzing the energy performance of residential buildings. The model was constructed on the basis of a feed-forward neural network which was optimized by a metaheuristic algorithm, namely the electrostatic discharge algorithm. The main findings can be drawn as follows:

- The hybrid model could analyze the building’s characteristics and reach an accurate understanding of the behavior of two energy parameters simultaneously, i.e., annual thermal energy demand and annual weighted average discomfort degree-hours. The correlation results for both  $D_{THE}$  and  $H_{DD}$  reached above 90% agreement between the actual data and the simulation results.
- Moreover, based on several accuracy representatives, the ESDA exhibited better performance compared to benchmark algorithms including future search algorithm, atom search optimization, and satin bowerbird optimization.
- A double-target formula was extracted from the proposed model for convenient calculations of the energy parameters.
- Based on this study, it is recommended to pursue the practical use of the ESDA to confirm its efficient analysis of building energy performance in real world applications such as optimizing air conditioning systems. This could provide insight into whether the proposed methodology would need some modifications and improvements that could be investigated in future relevant works.

**Author Contributions:** Data Curation, A.M.F., E.G., L.S.S., H.G. and B.A.; Formal Analysis, A.M.F., E.G., L.S.S., H.G. and B.A.; Investigation, A.M.F., E.G., L.S.S., H.G. and B.A.; Software, A.M.F., E.G., L.S.S., H.G. and B.A.; Visualization, A.M.F., E.G., L.S.S., H.G. and B.A.; Writing–Original Draft, A.M.F., E.G., L.S.S., H.G. and B.A.; Conceptualization, M.L.N.; Funding Acquisition, M.L.N.; Methodology, M.L.N.; Project Administration, M.L.N.; Resources, M.L.N.; Writing–Review & Editing, M.L.N. All authors have read and agreed to the published version of the manuscript.

**Funding:** This research received no funding.

**Institutional Review Board Statement:** Not applicable.

**Informed Consent Statement:** Not applicable.

**Data Availability Statement:** The data used in this research is taken from a study by Chegari, et al. [44] and is available in that study.

**Conflicts of Interest:** The authors declare no conflict of interest.

## References

1. Lu, C.; Zhu, R.; Yu, F.; Jiang, X.; Liu, Z.; Dong, L.; Hua, Q.; Ou, Z. Gear rotational speed sensor based on FeCoSiB/Pb (Zr, Ti) O<sub>3</sub> magnetoelectric composite. *Measurement* **2021**, *168*, 108409. [CrossRef]
2. Guo, L.; Ye, C.; Ding, Y.; Wang, P. Allocation of centrally switched fault current limiters enabled by 5G in transmission system. *IEEE Trans. Power Deliv.* **2020**, *36*, 3231–3241. [CrossRef]
3. Lu, C.; Zhou, H.; Li, L.; Yang, A.; Xu, C.; Ou, Z.; Wang, J.; Wang, X.; Tian, F. Split-core magnetoelectric current sensor and wireless current measurement application. *Measurement* **2022**, *188*, 110527. [CrossRef]
4. Lei, W.; Hui, Z.; Xiang, L.; Zelin, Z.; Xu-Hui, X.; Evans, S. Optimal remanufacturing service resource allocation for generalized growth of retired mechanical products: Maximizing matching efficiency. *IEEE Access* **2021**, *9*, 89655–89674. [CrossRef]
5. Hao, W.; Xie, J. Reducing diffusion-induced stress of bilayer electrode system by introducing pre-strain in lithium-ion battery. *J. Electrochem. Energy Convers. Storage* **2021**, *18*, 020909. [CrossRef]
6. Li, S.; Geng, Z. Bicriteria scheduling on an unbounded parallel-batch machine for minimizing makespan and maximum cost. *Inf. Process. Lett.* **2023**, *180*, 106343. [CrossRef]
7. Han, Y.; Xu, X.; Zhao, Y.; Wang, X.; Chen, Z.; Liu, J. Impact of consumer preference on the decision-making of prefabricated building developers. *J. Civ. Eng. Manag.* **2022**, *28*, 166–176. [CrossRef]
8. Han, Y.; Wang, L.; Kang, R. Influence of consumer preference and government subsidy on prefabricated building developer's decision-making: A three-stage game model. *J. Civ. Eng. Manag.* **2023**, *29*, 35–49. [CrossRef]
9. Han, Y.; Yan, X.; Piroozfar, P. An overall review of research on prefabricated construction supply chain management. *Eng. Constr. Archit. Manag.* **2022**. ahead-of-print. [CrossRef]
10. Hu, S.; Wang, J.; Hoare, C.; Li, Y.; Pauwels, P.; O'Donnell, J. Building energy performance assessment using linked data and cross-domain semantic reasoning. *Autom. Constr.* **2021**, *124*, 103580. [CrossRef]
11. Kim, D.D.; Suh, H.S. Heating and cooling energy consumption prediction model for high-rise apartment buildings considering design parameters. *Energy Sustain. Dev.* **2021**, *61*, 1–14. [CrossRef]
12. Dandotiya, B.; Sharma, H.K. Climate Change and Its Impact on Terrestrial Ecosystems. In *Research Anthology on Environmental and Societal Impacts of Climate Change*; IGI Global: Hershey, PA, USA, 2022; pp. 88–101.
13. Olu-Ajayi, R.; Alaka, H.; Sulaimon, I.; Sunmola, F.; Ajayi, S. Machine learning for energy performance prediction at the design stage of buildings. *Energy Sustain. Dev.* **2022**, *66*, 12–25. [CrossRef]
14. Lin, L.; Chen, C.; Wei, B.; Li, H.; Shi, J.; Zhang, J.; Huang, N. Residential electricity load scenario prediction based on transferable flow generation model. *J. Electr. Eng. Technol.* **2023**, *18*, 99–109. [CrossRef]
15. Do, H.; Cetin, K.S. Residential building energy consumption: A review of energy data availability, characteristics, and energy performance prediction methods. *Curr. Sustain. /Renew. Energy Rep.* **2018**, *5*, 76–85. [CrossRef]
16. Ding, Y.; Zhang, Q.; Yuan, T.; Yang, K. Model input selection for building heating load prediction: A case study for an office building in Tianjin. *Energy Build.* **2018**, *159*, 254–270. [CrossRef]
17. Lumbreras, M.; Garay-Martinez, R.; Arregi, B.; Martin-Escudero, K.; Diarce, G.; Raud, M.; Hagu, I. Data driven model for heat load prediction in buildings connected to District Heating by using smart heat meters. *Energy* **2022**, *239*, 122318. [CrossRef]
18. Qin, X.; Liu, Z.; Liu, Y.; Liu, S.; Yang, B.; Yin, L.; Liu, M.; Zheng, W. User OCEAN personality model construction method using a BP neural network. *Electronics* **2022**, *11*, 3022. [CrossRef]
19. Meng, Q.; Lai, X.; Yan, Z.; Su, C.-Y.; Wu, M. Motion planning and adaptive neural tracking control of an uncertain two-link rigid-flexible manipulator with vibration amplitude constraint. *IEEE Trans. Neural Netw. Learn. Syst.* **2021**, *33*, 3814–3828. [CrossRef]
20. Baduge, S.K.; Thilakarathna, S.; Perera, J.S.; Arashpour, M.; Sharafi, P.; Teodosio, B.; Shringi, A.; Mendis, P. Artificial intelligence and smart vision for building and construction 4.0: Machine and deep learning methods and applications. *Autom. Constr.* **2022**, *141*, 104440. [CrossRef]
21. Debrah, C.; Chan, A.P.; Darko, A. Artificial intelligence in green building. *Autom. Constr.* **2022**, *137*, 104192. [CrossRef]
22. Yegnanarayana, B. *Artificial Neural Networks*; PHI Learning Pvt. Ltd.: New Delhi, India, 2009.
23. Cho, J.H.; Moon, J.W. Integrated artificial neural network prediction model of indoor environmental quality in a school building. *J. Clean. Prod.* **2022**, *344*, 131083. [CrossRef]
24. Gerald, M.S.; Ghisi, E. Data-driven framework towards realistic bottom-up energy benchmarking using an Artificial Neural Network. *Appl. Energy* **2022**, *306*, 117960. [CrossRef]
25. Zhang, H.; Feng, H.; Hewage, K.; Arashpour, M. Artificial Neural Network for Predicting Building Energy Performance: A Surrogate Energy Retrofits Decision Support Framework. *Buildings* **2022**, *12*, 829. [CrossRef]

26. Gao, W.; Alsarraf, J.; Moayedi, H.; Shahsavari, A.; Nguyen, H. Comprehensive preference learning and feature validity for designing energy-efficient residential buildings using machine learning paradigms. *Appl. Soft Comput.* **2019**, *84*, 105748. [[CrossRef](#)]
27. Gupta, T.K.; Raza, K. Optimization of ANN architecture: A review on nature-inspired techniques. In *Machine Learning in Bio-Signal Analysis and Diagnostic Imaging*; Academic Press: Cambridge, MA, USA, 2019; pp. 159–182.
28. Hemeida, A.M.; Hassan, S.A.; Mohamed, A.-A.A.; Alkhalaf, S.; Mahmoud, M.M.; Senjyu, T.; El-Din, A.B. Nature-inspired algorithms for feed-forward neural network classifiers: A survey of one decade of research. *Ain Shams Eng. J.* **2020**, *11*, 659–675. [[CrossRef](#)]
29. Chou, J.-S.; Ngo, N.-T. Time series analytics using sliding window metaheuristic optimization-based machine learning system for identifying building energy consumption patterns. *Appl. Energy* **2016**, *177*, 751–770. [[CrossRef](#)]
30. Moayedi, H.; Mosavi, A. Suggesting a stochastic fractal search paradigm in combination with artificial neural network for early prediction of cooling load in residential buildings. *Energies* **2021**, *14*, 1649. [[CrossRef](#)]
31. Liang, R.; Le-Hung, T.; Nguyen-Thoi, T. Energy consumption prediction of air-conditioning systems in eco-buildings using hunger games search optimization-based artificial neural network model. *J. Build. Eng.* **2022**, *59*, 105087. [[CrossRef](#)]
32. Alkhazaleh, H.A.; Nahi, N.; Hashemian, M.H.; Nazem, Z.; Shamsi, W.D.; Nehdi, M.L. Prediction of Thermal Energy Demand Using Fuzzy-Based Models Synthesized with Metaheuristic Algorithms. *Sustainability* **2022**, *14*, 14385. [[CrossRef](#)]
33. Le, L.T.; Nguyen, H.; Dou, J.; Zhou, J. A comparative study of PSO-ANN, GA-ANN, ICA-ANN, and ABC-ANN in estimating the heating load of buildings' energy efficiency for smart city planning. *Appl. Sci.* **2019**, *9*, 2630. [[CrossRef](#)]
34. Tien Bui, D.; Moayedi, H.; Anastasios, D.; Kok Foong, L. Predicting heating and cooling loads in energy-efficient buildings using two hybrid intelligent models. *Appl. Sci.* **2019**, *9*, 3543. [[CrossRef](#)]
35. Guo, Z.; Moayedi, H.; Foong, L.K.; Bahiraei, M. Optimal modification of heating, ventilation, and air conditioning system performances in residential buildings using the integration of metaheuristic optimization and neural computing. *Energy Build.* **2020**, *214*, 109866. [[CrossRef](#)]
36. Jahanafroozi, N.; Shokrpour, S.; Nejati, F.; Benjeddou, O.; Khordehbinan, M.W.; Marani, A.; Nehdi, M.L. New Heuristic Methods for Sustainable Energy Performance Analysis of HVAC Systems. *Sustainability* **2022**, *14*, 14446. [[CrossRef](#)]
37. Seyedashraf, O.; Mehrabi, M.; Akhtari, A.A. Novel approach for dam break flow modeling using computational intelligence. *J. Hydrol.* **2018**, *559*, 1028–1038. [[CrossRef](#)]
38. Zhao, Y.; Foong, L.K. Predicting Electrical Power Output of Combined Cycle Power Plants Using a Novel Artificial Neural Network Optimized by Electrostatic Discharge Algorithm. *Measurement* **2022**, *198*, 111405. [[CrossRef](#)]
39. Mu'azu, M.A. Hybridized artificial neural network with metaheuristic algorithms for bearing capacity prediction. *Ain Shams Eng. J.* **2022**, *14*, 101980. [[CrossRef](#)]
40. Elsis, M. Future search algorithm for optimization. *Evol. Intell.* **2019**, *12*, 21–31. [[CrossRef](#)]
41. Zhao, W.; Wang, L.; Zhang, Z. Atom search optimization and its application to solve a hydrogeologic parameter estimation problem. *Knowl.-Based Syst.* **2019**, *163*, 283–304. [[CrossRef](#)]
42. Moosavi, S.H.S.; Bardsiri, V.K. Satin bowerbird optimizer: A new optimization algorithm to optimize ANFIS for software development effort estimation. *Eng. Appl. Artif. Intell.* **2017**, *60*, 1–15. [[CrossRef](#)]
43. Klein, S.; Beckman, W.; Mitchell, J.; Duffie, J.; Duffie, N.; Freeman, T.; Mitchell, J.; Braun, J.; Evans, B.; Kummer, J. *TRNSYS 17: A Transient System Simulation Program*, Solar Energy Laboratory; University of Wisconsin: Madison, WI, USA, 2010.
44. Chegari, B.; Tabaa, M.; Simeu, E.; Moutaouakkil, F.; Medromi, H. Multi-objective optimization of building energy performance and indoor thermal comfort by combining artificial neural networks and metaheuristic algorithms. *Energy Build.* **2021**, *239*, 110839. [[CrossRef](#)]
45. Safayenikoo, H.; Nejati, F.; Nehdi, M.L. Indirect Analysis of Concrete Slump Using Different Metaheuristic-Empowered Neural Processors. *Sustainability* **2022**, *14*, 10373. [[CrossRef](#)]
46. Mehrabi, M.; Pradhan, B.; Moayedi, H.; Alamri, A. Optimizing an adaptive neuro-fuzzy inference system for spatial prediction of landslide susceptibility using four state-of-the-art metaheuristic techniques. *Sensors* **2020**, *20*, 1723. [[CrossRef](#)]
47. Kashan, A.H. A new metaheuristic for optimization: Optics inspired optimization (OIO). *Comput. Oper. Res.* **2015**, *55*, 99–125. [[CrossRef](#)]
48. Bouchekara, H.R. Electrostatic discharge algorithm: A novel nature-inspired optimisation algorithm and its application to worst-case tolerance analysis of an EMC filter. *IET Sci. Meas. Technol.* **2019**, *13*, 491–499. [[CrossRef](#)]
49. Masugi, M. Multiresolution analysis of electrostatic discharge current from electromagnetic interference aspects. *IEEE Trans. Electromagn. Compat.* **2003**, *45*, 393–403. [[CrossRef](#)]
50. Hassoun, M.H. *Fundamentals of Artificial Neural Networks*; MIT Press: Cambridge, MA, USA, 1995.
51. Reed, R.; MarksII, R.J. *Neural Smithing: Supervised Learning in Feedforward Artificial Neural Networks*; MIT Press: Cambridge, MA, USA, 1999.
52. Moayedi, H.; Mehrabi, M.; Mosallanezhad, M.; Rashid, A.S.A.; Pradhan, B. Modification of landslide susceptibility mapping using optimized PSO-ANN technique. *Eng. Comput.* **2019**, *35*, 967–984. [[CrossRef](#)]
53. Wu, D.; Foong, L.K.; Lyu, Z. Two neural-metaheuristic techniques based on vortex search and backtracking search algorithms for predicting the heating load of residential buildings. *Eng. Comput.* **2022**, *38*, 647–660. [[CrossRef](#)]

54. Almutairi, K.; Algarni, S.; Alqahtani, T.; Moayedi, H.; Mosavi, A. A TLBO-Tuned Neural Processor for Predicting Heating Load in Residential Buildings. *Sustainability* **2022**, *14*, 5924. [[CrossRef](#)]
55. Rastbod, S.; Rahimi, F.; Dehghan, Y.; Kamranfar, S.; Benjeddou, O.; Nehdi, M.L. An Optimized Machine Learning Approach for Forecasting Thermal Energy Demand of Buildings. *Sustainability* **2023**, *15*, 231. [[CrossRef](#)]
56. Mehrabi, M.; Moayedi, H. Landslide susceptibility mapping using artificial neural network tuned by metaheuristic algorithms. *Environ. Earth Sci.* **2021**, *80*, 804. [[CrossRef](#)]
57. Zhang, C.; Ali, A.; Sun, L. Investigation on low-cost friction-based isolation systems for masonry building structures: Experimental and numerical studies. *Eng. Struct.* **2021**, *243*, 112645. [[CrossRef](#)]
58. Zhang, Z.; Li, W.; Yang, J. Analysis of stochastic process to model safety risk in construction industry. *J. Civ. Eng. Manag.* **2021**, *27*, 87–99. [[CrossRef](#)]
59. Guo, C.; Ye, C.; Ding, Y.; Wang, P. A multi-state model for transmission system resilience enhancement against short-circuit faults caused by extreme weather events. *IEEE Trans. Power Deliv.* **2020**, *36*, 2374–2385. [[CrossRef](#)]
60. Lin, C.; Wang, J. Metaheuristic-designed systems for simultaneous simulation of thermal loads of building. *Smart Struct. Syst.* **2022**, *29*, 677–691.
61. Nguyen, H.; Mehrabi, M.; Kalantar, B.; Moayedi, H.; Abdullahi, M.A.M. Potential of hybrid evolutionary approaches for assessment of geo-hazard landslide susceptibility mapping. *Geomat. Nat. Hazards Risk* **2019**, *10*, 1667–1693. [[CrossRef](#)]
62. Zhou, G.; Moayedi, H.; Foong, L.K. Teaching–learning-based metaheuristic scheme for modifying neural computing in appraising energy performance of building. *Eng. Comput.* **2021**, *37*, 3037–3048. [[CrossRef](#)]

**Disclaimer/Publisher’s Note:** The statements, opinions and data contained in all publications are solely those of the individual author(s) and contributor(s) and not of MDPI and/or the editor(s). MDPI and/or the editor(s) disclaim responsibility for any injury to people or property resulting from any ideas, methods, instructions or products referred to in the content.